LA-UR-18-28671 (Accepted Manuscript)

# Synthesis of Aromatic Anion Exchange Membranes by Friedel–Crafts Bromoalkylation and Cross-Linking of Polystyrene Block Copolymers

Jeon, Jong Yeob; Kim, Yu Seung; Mohanty, Angela D.; Tian, Ding; Park, Sungmin; Saikia, Nayan; Hickner, Michael; Ryu, Chang; Tuckerman, Mark E.; Paddison, Stephen J.; Bae, Chulsung; Maurya, Sandipkumar



**To be published in:** Macromolecules

**DOI to publisher's version:** 10.1021/acs.macromol.8b02355

**Permalink to record:** http://permalink.lanl.gov/object/view?what=info:lanl-repo/lareport/LA-UR-18-28671

# Synthesis of Aromatic Anion Exchange Membranes by Friedel-Crafts *Bromoalkylation* and Crosslinking of Polystyrene Block Copolymers

Jong Yeob Jeon,[†] Sungmin Park,[†] Junyoung Han,[†] Sandip Maurya,[▽] Angela D. Mohanty,[†] Ding Tian,[†] Nayan Saikia,[‡] Michael A. Hickner,[‡] Chang Y. Ryu,[†] Mark E. Tuckerman,[§,∥,⊥] Stephen J. Paddison,[#] Yu Seung Kim,[▽] and Chulsung Bae*[,†,±]

[†]Department of Chemistry and Chemical Biology, Rensselaer Polytechnic Institute, 110 8th Street, Troy, New York 12180, United States

[±]Department of Chemical and Biological Engineering, Rensselaer Polytechnic Institute, 110 8th Street, Troy, New York 12180, United States

[‡]Department of Materials Science and Engineering, The Pennsylvania State University, University Park, Pennsylvania 16802, United States

[#]Department of Chemical & Biomolecular Engineering, University of Tennessee, Knoxville, Tennessee 37996, United States

§Department of Chemistry, New York University, New York, New York 10003, United States

∥Courant Institute of Mathematical Sciences, New York University, New York, New York 10012, United States

[⊥]NYU-ECNU Center for Computational Chemistry, NYU Shanghai, 3663 Zhongshan Road North, Shanghai 200062, China

[▽]MPA-11: Materials Synthesis and Integrated Devices, Los Alamos National Laboratory, Los Alamos, New Mexico 87545, United States

**ABSTRACT:** Elastomeric anion exchange membranes (AEMs) were prepared by acid-catalyzed Friedel-Crafts alkylation of the polystyrene block of polystyrene-*b*-poly(ethylene-*co*-butylene)-*b*-polystyrene (SEBS) using bromoalkylated *tertiary* alcohols and triflic acid as a catalyst, followed by amination with trimethylamine. This simple one-step bromoalkylation allowed convenient control of both the degree of functionalization and cation tether length by changing the molar ratio and the structure of the bromoalkylated *tertiary* alcohol. The resulting quaternary ammonium-functionalized ionic triblock SEBS copolymers showed a microphase-separated morphology on the 35 nm length scale. A series of AEMs with different ion exchange capacities and ion tether lengths were systematically investigated by comparing swelling and anion conductivity. Since the SEBS AEMs showed high swelling and low dimensional stability in water due to the rubbery nature of SEBS, the hard segment PS units were crosslinked by 1,6-hexanediamine for practical use. The crosslinking of SEBS AEMs reduced water uptake significanlty (e.g., 155% *vs.* 28%), and enhanced their mechanical properties. Because the backbone of the SEBS AEMs are composed of all carbon-carbon bonds, they showed good alkaline stability, preserving their IEC and $OH^-$ conductivity after testing in a 1 M NaOH solution at 80°C for 500 hours. Alkaline membrane fuel cell performance was evaluated with the crosslinked SEBS AEM, and a peak power density of 520 mW/cm$^2$ was achieved at 60°C under $H_2/O_2$ conditions.

## INTRODUCTION

Anion exchange membrane (AEM) fuel cells operating at high pH can offer several benefits in comparison to proton exchange membrane (PEM) fuel cells operating under acidic conditions: (a) faster kinetics for the oxygen reduction reaction in alkaline conditions; and (b) the possible use of nonprecious metal electrocatalysts due to low rates of corrosion at high pH. Unfortunately, these potential benefits have not been realized in long-lifetime durable fuel cells because of the drawbacks of currently available AEMs, which include poor chemical stability under alkaline operating conditions, insufficient mechanical properties, low hydroxide ion conductivity, and the lack of convenient synthetic methods for rapid synthesis of these materials.[1-6]

The durability of AEMs is strongly dependent on the chemical stability of the polymer backbone. For example, poly(arylene ether)s, the most common backbone structure of AEMs,[7-12] contain aryl ether linkages and the backbone is prone to undergo chain scission in alkaline conditions through nucleophilic attack by the hydroxide ion,[13-14] significantly reducing the AEM durability. Therefore, it is desirable to design AEMs in which the polymer backbone does not contain heteroatoms. Recently, a number of reported AEMs made of all carbon-based backbones support that this AEM design concept is appropriate for enhancing alkaline stability.[15-19] Ion conductivity is dependent on a number of factors including the density of ionic groups in the

**Scheme 1. Synthetic Route for QA-functionalized SEBS *via* Friedel-Crafts Bromoalkylation (n=3-5; R=$(CH_2)_6$; x=degree of functionalization; y=degree of crosslinking)**

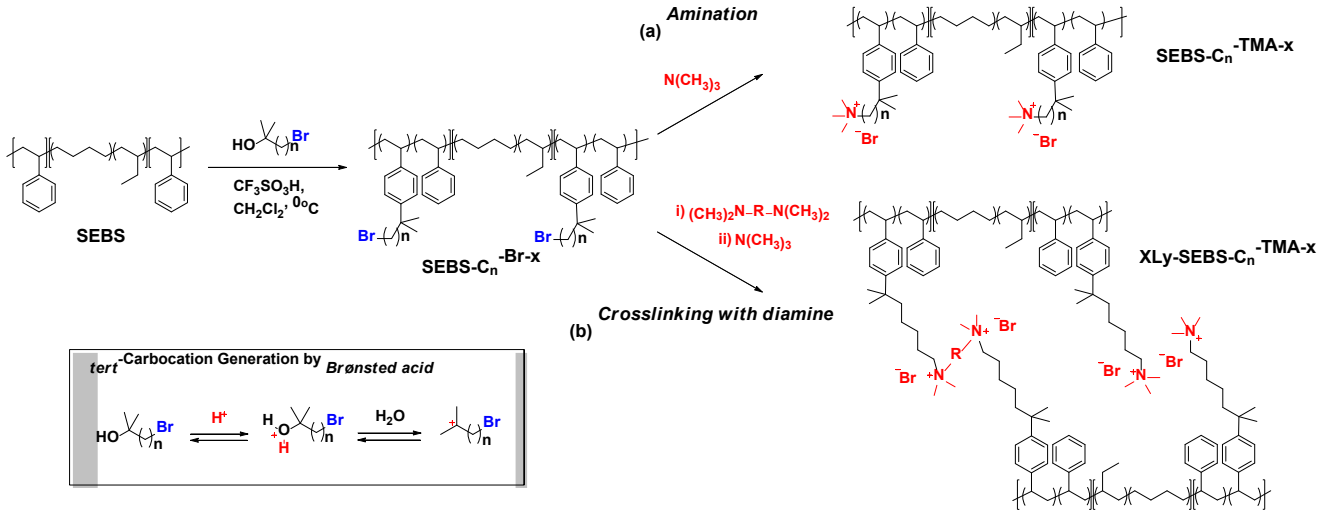


material and the distribution of the ionic groups in the material's phase-separated morphology. The former is typically represented by ion exchange capacity (IEC; in mequiv./g) and the latter is related to polymer architecture which determines the formation of percolating ionic domains for efficient ion transport.[20-21] Various ion exchange membranes with flexible side chains were suggested for the formation of hydrophilic-hydrophobic phase-separated morphology in both PEMs and AEMs, which promotes ion conductivity under conditions of minimal hydration.[22-26]

In designing polymer candidates for AEM applications, we envision that polystyrene-*b*-poly(ethylene-*co*-butylene)-*b*-polystyrene (SEBS) may serve as a promising AEM backbone because: (a) it is composed of all carbon-carbon bonds affording good polymer backbone stability against hydroxide attack, and (b) the thermodynamic immiscibility of the two blocks in SEBS is known to induce nanoscale phase-separated morphology which will increase the ionic conductivity of the material. Since SEBS is a commercially available thermoplastic elastomer, selective functionalization of the polystyrene (PS) block can create a new class of elastic ionic block copolymer AEMs with tunable microstructures. However, there have been very few reports of SEBS-based AEMs because chloromethylation, the most frequently used method of aromatic ring functionalization for AEM synthesis, does not facilitate incorporation of a high degree of functional groups into the PS block in SEBS due to gelation during synthesis.[27-29]

To avoid gelation during chloromethylation, Bae and coworkers have reported controlled functionalization of SEBS *via* C-H borylation and Suzuki coupling reactions.[30] A high degree of functionalization (DF; up to 90% of the PS repeating unit) could be achieved, and quaternary ammonium (QA) pendant structures and cation tether lengths could be tuned by choosing appropriate amine-containing aryl halides for Suzuki coupling. However, the use of expensive transition metal catalysts, such as Ir and Pd, and the need for reactions in a glovebox can be a major barrier to scale-up and broader application of this synthetic method. Additionally, a SEBS-based AEM prepared by Friedel-Crafts acylation using $AlCl_3$ catalyst, subsequent ketone reduction, and nucleophilic quaternization reaction was reported,[31] similar to the approach taken by Hibbs for polyphenylene-based AEMs.[32] However, the requirement of extra reduction step of C=O to $CH_2$ is not desirable in the context of economical synthesis. Therefore, new methods to achieve similar structures are highly desirable.

We report here a new synthetic method for QA functionalization of aromatic polymers using bromoalkylated *tertiary* alcohols (i.e. bromoalkylation), a type of acid-catalyzed Friedel-Crafts reaction, followed by amination. In this method, the alkyl tether length and DF in the PS block can be conveniently tuned by changing the chemical structure and molar ratio of the bromoalkyl *tertiary* alcohol. After amination with trimethylamine, a number of alkyltrimethylammonium (TMA)-functionalized SEBS AEMs were obtained. The overall synthetic route is shown in Scheme 1.

## RESULTS AND DISCUSSION

**Preparation of SEBS AEMs.** The aromatic rings of SEBS ($M_n$ = 105,000 g/mol, and $M_w/M_n$ = 1.04) with 18 mol% (30 wt.%, 25 vol.%) PS block were functionalized *via* acid-catalyzed Friedel-Crafts bromoalkylation. As the *tertiary* alcohol is protonated by a Brønsted acid, it loses water as a byproduct and forms a *tertiary* carbocation intermediate, which can readily react with the π electrons of the aromatic rings to generate bromoalkylated SEBS (see Scheme 1; SEBS-$C_n$-Br-x, where n indicates the number of carbons in the tether chain and x indicates the DF in mol%). Various organic acids including sulfuric acid, methanesulfonic acid, trifluoroacetic acid, *para*-toluenesulfonic acid, and trifluoromethanesulfonic (triflic) acid were screened, and we found that triflic acid is the most effective acid catalyst for this reaction. Slightly more than 1 eq. of acid (1.1–1.2 eq.) relative to the *tert*-alcohol reagent was required because the reaction byproduct water is also readily protonated by triflic acid, thus reducing its reactivity. Excessive addition of triflic acid caused gelation of the polymer. Since the reaction is exothermic, the reaction was conducted at 0°C.

The DF of the PS block was easily controlled by changing the molar ratio of the *tert*-alcohol reagent to the aromatic ring of the PS block. For example, a reaction with 0.5 eq. of the bromoalkylated *tert*-alcohol relative to the PS block resulted in 50 mol% DF while a reaction with 1.0 eq. of the alcohol reagent resulted 80 mol% DF. A maximum of 95 mol% DF could be achieved for the PS block of SEBS when 2.0 eq. of the *tert*-

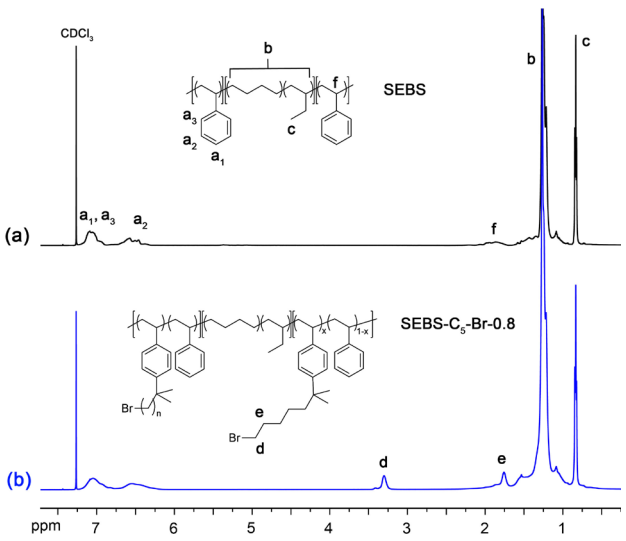


**Figure 1.** $^{1}$H MNR spectra of (a) pristine SEBS and (b) bromoalkylated SEBS-C$_5$-Br-0.8.

alcohol was employed, however, the resulting QA membrane after the amination step (i.e. SEBS-C$_5$-TMA-0.95) was dimensionally unstable. SEBS is a thermoplastic elastomer comprised of a soft poly(ethylene-*co*-butylene) (PEB) block and a hard PS block. After incorporation of QA groups into the PS block, the water molecules absorbed in the PS block act as a plasticizer to soften the hard block, resulting in a membrane with swelling and poor mechanical strength. Thus, some balance between IEC and mechanical properties is required.

DFs were calculated by comparing proton integration values of the $^{1}$H NMR spectra. In the $^{1}$H NMR spectrum of pristine SEBS (Figure 1a), the integration ratio of Ar-***H***$_5$ (peak **a**$_{1\text{-}3}$ at 6.3–7.2 ppm), butylene-C***H***$_3$ (peak **c** at 0.7–0.9 ppm), and the other C***H***$_2$ and C***H*** (peak **b** at 1.0–2.0 ppm) indicates that the molar ratios of styrene, ethylene, and butylene contents are 18, 51 and 31 mol%, respectively. After Friedel-Crafts reaction with bromoalkylated alcohols, new proton signals of -C***H***$_2$Br at 3.2–3.3 ppm (peak **d** in Figure 1b) along with the -C***H***$_2$CH$_2$Br signal (peak **e** in Figure 1b) appeared. DFs were calculated from the integration ratio of the -C***H***$_2$Br signal of the functionalized SEBS (peak **d**) and the butylene-C***H***$_3$ signal of the pristine SEBS (peak **c**).

The tether length between the cation head group and the polymer backbone was controlled by modifying the alkyl chain length (n of Scheme 1) in the structure of brominated *tert*-alcohol. We synthesized a series of bromoalkylated SEBSs with different tether lengths (n = 3–5) and different DFs (50 and 80 mol% of PS block). Functionalization with a shorter tether length (n = 1 and 2) was unsuccessful likely due to instability of the carbocation intermediate when the bromine is located too close to the carbocation center.

After the acid-catalyzed Friedel-Crafts reaction, we noticed the molecular weights of the functionalized SEBS were significantly increased while preserving a narrow polydispersity index (Table S1 and Figure S1). To clarify what caused molecular weight change, we conducted the same Friedel-Crafts bromoalkylation reaction using a monodisperse PS sample ($M_n$ = 81 kg/mol, $M_w/M_n$ = 1.03). After the functionalization, the $M_n$ of PS with 60 mol% DF slightly increased to 104 kg/mol due to changes in hydrodynamic volume of the polymer while maintaining $M_w/M_n$ = 1.04 (Figure 2). The results of the PS bromoalkylation suggest that the molecular weight change in SEBS bromoalkylation originated from the PEB block, not from the aromatic block. Note that SEBS is synthesized by hydrogenation of polystyrene-*b*-polybutadiene-*b*-polystyrene (SBS). Since it is difficult to completely hydrogenate every double bond in SBS, a small amount of remaining double bonds might be protonated under the acidic Friedel-Crafts reaction conditions to form a carbocation in the PEB block,[33] which may have reacted with the aromatic rings of the PS chains and contributed

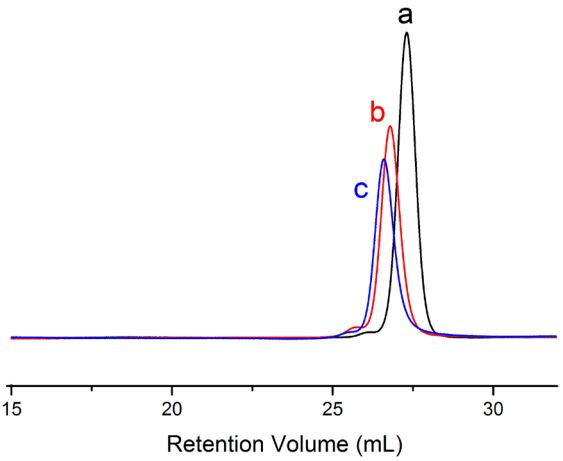


**Figure 2.** SEC curves of (a) pristine polystyrene ($M_n$=81 kg/mol, PDI=1.03), (b) 60 mol% bromoalkylated PS ($M_n$=104 kg/mol, PDI=1.04), and (c) 70 mol% bromoalkylated polystyrene ($M_n$=109 kg/mol, PDI=1.06).

**Table 1. Ion Exchange Capacity (IEC), water uptake, and ion conductivity of TMA-functionalized SEBS AEMs and cross-linked SEBS AEMs**

| Samples | IEC(mequiv./g) | | WU[c] (wt. %) | λ[d] | In-plane swelling[e] (%) | $Cl^-$ σ (mS/cm) 60 °C | $OH^-$ σ (mS/cm)[f] | | |
|---|---|---|---|---|---|---|---|---|---|
| | $^1$H NMR[a] | Titration[b] | | | | | 30 °C | 60 °C | 80 °C |
| SEBS-$C_3$-TMA-0.5 | 1.12 | 1.09 | 110 (± 5) | 58 | 30 | 18 | 21 | 36 | 50 |
| SEBS-$C_4$-TMA-0.5 | 1.10 | 1.12 | 123 (± 6) | 66 | 26 | 19 | 22 | 37 | 55 |
| SEBS-$C_5$-TMA-0.5 | 1.09 | 1.02 | 120 (± 5) | 65 | 23 | 18 | 20 | 35 | –[g] |
| SEBS-$C_3$-TMA-0.8 | 1.62 | 1.55 | 150 (± 10) | 53 | 31 | 30 | 47 | 72 | 93 |
| SEBS-$C_4$-TMA-0.8 | 1.58 | 1.51 | 155 (± 10) | 56 | 32 | 28 | 36 | 60 | –[g] |
| SEBS-$C_5$-TMA-0.8 | 1.55 | 1.45 | 155 (± 10) | 56 | 26 | 20 | 23 | 41 | –[g] |
| XL20-SEBS-$C_5$-TMA-0.8[h] | 1.54 | 1.46 | 70 (± 5) | 25 | 15 | 17 | 30 | 42 | 62 |
| XL60-SEBS-$C_5$-TMA-0.8[h] | 1.52 | 1.47 | 46 (± 3) | 17 | 13 | 15 | 33 | 45 | 65 |
| XL100-SEBS-$C_5$-TMA-0.8[h] | 1.50 | 1.46 | 28 (± 2) | 10 | 10 | 13 | 29 | 41 | 65 |

[a]NMR based IECs are expected values of $OH^-$ form of AEMs calculated from the concentrations of bromoalkyl group in $^1$H NMR spectrum of SEBS-$C_n$-Br-x. [b]Titrated IECs values of SEBS AEMs from Mohr titration method (average of two experiments). [c]Water uptake was measured at r.t. in $OH^-$ Form (average of two measurements). [d]The hydration number. [e]Swelling was measured at r.t. in $OH^-$ form. [f]All $OH^-$ σ were measured in water under argon atomosphere. [g]$OH^-$ σ were not measurable due to mechanical instability of the membrane at 80 °C. [h]Crosslinked membranes of SEBS-$C_5$-TMA-0.8; XLy-SEBS-$C_5$-TMA-0.8, where y indicates degree of cross-linking calculated by the N:Br ratio of added crosslinking agent, *N*,*N*,*N*',*N*'-tetramethyl-1,6-hexanediamine, to –$CH_2$Br group.

to the increase of molecular weight (see Figure S2 of the Supporting Information for proposed mechanism of *intermolecular linking* side reaction). Although the functionalization affected molecular weights of SEBS, the bromoalkylated SEBSs are readily soluble in organic solvents such as THF, chloroform and toluene.

After amination of the bromoalkyl side chain of SEBS-$C_n$-Br-x with trimethylamine, the TMA-functionalized polymers were not soluble in any solvent. Hence, we cast films of SEBS-$C_n$-Br-x from a 5 wt.% toluene solution on a glass plate (membrane thickness: 40-50 μm), and subsequent amination was performed by immersing the membranes in an aqueous trimethylamine solution (Scheme 1a). Completion of the reaction was confirmed by determining the IEC with titration and infrared spectroscopy (Figures S3–S5 of Supporting Information). All SEBS-$C_n$-TMA-x membranes listed in Table 1 were flexible, elastomeric, colorless and transparent.

**Membrane Properties.** Representative AEM properties including IEC, water uptake (WU), in-plane swelling ratio and ion conductivity of the TMA-functionalized SEBSs are summarized in Table 1. The NMR IECs were calculated from the DF of Friedel-Crafts bromoalkylation with the assumption that every bromoalkyl side group in the precursor polymer was converted to QA by amination. For 50% DF of the PS block, the NMR IEC values are 1.12, 1.10, and 1.09 mequiv./g with different tether lengths of $C_3$, $C_4$, and $C_5$, respectively. Similarly, 80% DF of the PS block afforded NMR IECs of 1.62, 1.58, and 1.55 mequiv./g with tether lengths of $C_3$, $C_4$, and $C_5$, respectively. The titrated IEC values from SEBS-$C_n$-TMA-x agree well the NMR-based IECs confirming that the amination with trimethylamine was quantitative.

As shown in entries 1–6 of Table 1, SEBS-$C_n$-TMA-x membranes showed relatively high WU and swelling ratio compared to typical AEMs because of the rubbery nature of the SEBS backbone. A high degree of QA incorporation into the PS block induced plasticization of the hard domain and softened the membranes further. WUs in the range of 110–123 wt.% were observed for SEBS-based AEMs with 50% DF while 150–155 wt.% WU was observed for 80% DF polymers. Hydration numbers (λ) of the SEBS AEMs were between 53–66. Ion conductivity of the SEBS AEMs was mainly dependent on the DF (and the resulting IEC) and tether length. While 50% DF QA polymers (SEBS-$C_n$-TMA-0.5) showed similar ion conductivity regardless of the tether length, 80% DF polymer samples (SEBS-$C_n$-TMA-0.8) clearly showed a trend where SEBS AEM samples with a shorter tether length displayed higher conductivity. For example, $OH^-$ conductivities of SEBS-$C_n$-TMA-0.8 were 72, 60, and 41 mS/cm at 60 °C in liquid water with the tether lengths of $C_3$, $C_4$, and $C_5$, respectively. These $OH^-$ conductivity values are about two times higher than the measured $Cl^-$ conductivities. Unfortunately, due to the soft mechanical properties of SEBS-based AEMs, we were not able to measure reliable $OH^-$ conductivity at 80 °C for certain samples with the longer tether lengths (footnote g in Table 1).

In tensile strength measurements at 50% relative humidity and 50 °C, all SEBS AEM samples did not reach the breaking point until the instrument limit (350%-400% elongation).[34] The tensile stress of SEBS-$C_5$-TMA-0.8 at the point of 350% elongation was 3.9 MPa (Figure S6 of the Supporting Information). Compared to AEMs made of rigid aromatic polymer backbones with a comparable IEC (*e.g.* poly(arylene ether sulfone), 1.8 mequiv/g; 39 MPa ultimate tensile stress and 30% strain at break),[13] the SEBS AEMs showed a lower tensile strength and a higher elongation. Due to high water uptake and the rubbery nature of backbone, mechanical properties of these SEBS AEMs are not sufficient for the practical application of AEM

fuel cells. Therefore, reinforcement by crosslinking was explored for the practical use the materials.

**Crosslinked SEBS AEMs.** Crosslinking is a convenient method for reducing swelling of the membrane in water and improving the physical properties of soft materials. There have been many examples of crosslinked AEMs prepared by various methods including thermal crosslinking,[35] use of 1,6-hexanediamine as crosslinker,[36-38] thiol-ene click chemistry,[39-40] and olefin methathesis.[41] When chloromethylated SEBS was quaternized/crosslinked with *N*,*N*,*N*',*N*'-tetramethyl-1,6-hexanediamine (TMHDA), the crosslinked membranes afforded enhanced mechanical properties.[42-43] We adopted this concept for crosslinking of the *bromoalkylated* SEBS; SEBS-$C_5$-Br-0.8 was crosslinked with TMHDA during solvent casing of the membrane followed by quaternization of residual bromine group by trimethylamine (Scheme 1b). The degree of crosslinking was controlled by adjusting the amount of TMHDA relative to $-CH_2Br$ (XLy-SEBS-$C_5$-TMA-0.8, where y indicates degree of crosslinking estimated by molar ratio of the added nitrogen of TMHDA to $-CH_2Br$).

As the degree of crosslinking was increased, water uptake and in-plane swelling were significantly reduced (entries 7–9 of Table 1). The water uptake values were decreased from 155% to 70%, 46%, and 28% as degree of crosslinking increased from 0% to 20%, 60% and 100%, respectively. In-plane swelling ratios were 26%, 15%, 13%, and 10% for SEBS-$C_5$-TMA-0.8 with 0%, 20%, 60% and 100% degree of crosslinking, respectively. While we could not measure reliable $OH^-$ conductivity of SEBS-$C_5$-TMA-0.8 at 80°C (footnote g in entry 6 of Table 1), all crosslinked membranes of SEBS-$C_5$-TMA-0.8 showed stable $OH^-$ conductivity at that temperature, confirming that the crosslinking process greatly enhanced the dimensional stability of the SEBS AEM samples. Mechanical strength also improved after crosslinking. The maximum tensile stress of XL100-SEBS-$C_5$-TMA-0.8 was 7.0 MPa while the corresponding un-crosslinked membrane has tensile stress of 3.9 MPa (Figure S8 of the Supporting Information). Even after crosslinking, SEBS membranes still preserved elasticity and did not break when stretched up to 350%. Ion conductivity was not negatively affected by crosslinking. Overall, the crosslinking of SEBS AEMs produced dimensionally stable, elastic membrane materials without sacrificing hydroxide conductivity.

**Alkaline Stability Test.** Alkaline stability of the SEBS AEMs was evaluated by immersing the membranes in 1 M NaOH solution at 80 °C and measureing changes in titrated IEC, $OH^-$ conductivity, elemental analysis, mechanical properties, and morphology. As shown in Table 2, the titrated IEC and $OH^-$ conductivity of all membranes were preserved after the 500-hour test, indicating that they have excellent chemical stability

**Table 2. Titrated IEC and $OH^-$ conductivity before and after alkaline stability test**

| Samples | Titrated IEC (mequiv/g)[a] | | $OH^-$ σ (mS/cm) 60 °C[b] | |
|---|---|---|---|---|
| | 0 h | 500 h[c] | 0 h | 500 h[c] |
| SEBS-$C_3$-TMA-0.5 | 1.09 | 1.10 | 36 | 40 |
| SEBS-$C_4$-TMA-0.5 | 1.12 | 1.12 | 37 | 42 |
| SEBS-$C_5$-TMA-0.5 | 1.02 | 1.04 | 35 | 38 |
| SEBS-$C_3$-TMA-0.8 | 1.55 | 1.50 | 72 | 70 |
| SEBS-$C_4$-TMA-0.8 | 1.51 | 1.52 | 60 | 58 |
| SEBS-$C_5$-TMA-0.8 | 1.41 | 1.39 | 41 | 43 |
| XL20-SEBS-$C_5$-TMA-0.8 | 1.46 | 1.45 | 42 | 43 |
| XL60-SEBS-$C_5$-TMA-0.8 | 1.47 | 1.45 | 45 | 44 |
| XL100-SEBS-$C_5$-TMA-0.8 | 1.46 | 1.48 | 41 | 40 |

[a]Titrated IEC values from the Mohr titration method (average of two experiments). [b]All $OH^-$ σ were measured in water under an argon atmosphere (average of two experiments). [c]After alkaline test in 1 M NaOH Solution at 80 °C for 500 hr.

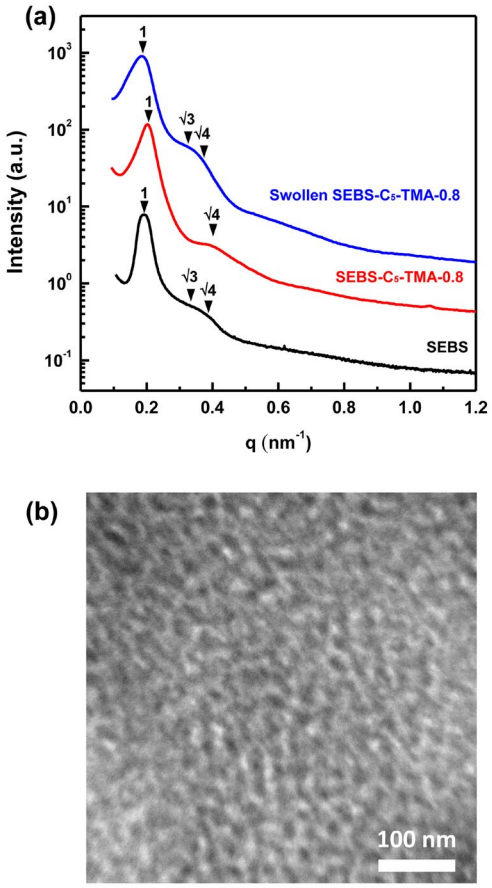


**Figure 3.** (a) SAXS profiles for SEBS and SEBS-$C_5$-TMA-0.8 membrane and (b) TEM image of SEBS-$C_5$-TMA-0.8 membrane.

under high pH conditions. If cation degradation by Hoffman elimination had occurred during the alkaline stability test, we would expect a decrease in the percentage of N (and associated Cl) in elemental analysis as it loses trimethylamine as a byproduct. However, the fact that we did not observe any significant difference in elemental analysis data before and after the stability test validates these samples' good alkaline stability (Table S3). Deterioration of mechanical properties during high pH degradation testing at elevated temperatures can be a major bottleneck for deploying these materials in practical electrochemical energy conversion devices. As shown in Figure S9–S13 of the Supporting Information, TMA-functionalized SEBSs (both uncrosslinked and crosslinked samples) showed no changes in tensile strength and elongation at break after the alkaline stability test, suggesting that these elastic membranes can endure harsh alkaline conditions with no degradation in their mechanical integrity. Additionally, there was no noticeable morphological change after the alkaline stability test (Figure S14). The SEBS-based AEMs were also stable under $O_2$ saturated alkaline conditions. We conducted additional alkaline stability tests by immersing the SEBS-$C_5$-TMA-0.8 sample in $O_2$ saturated 1M NaOH solution at 80 °C, and no change was observed in titrated IEC and $OH^-$ conductivity after 100 hours (Table S4 of Supporting Information).

**Morphological Characterization of SEBS AEMs.** The microphase-separated morphology of SEBS AEMs was investigated by small-angle X-ray scattering (SAXS) and transmission electron microscopy (TEM). Figure 3a shows the 1D intensity profiles of the SAXS data for pristine SEBS and SEBS-$C_5$-TMA-0.8 membranes (dry and hydrated forms) as a function of the scattering vector ($q = (4\pi/\lambda)\sin(\theta/2)$), where θ and $\lambda$ represent the scattering angle and wave-length of x-ray beam, respectively. The SAXS scattering peaks with $q/q^*$ ratios of 1, √3, √4, where $q^*$ is the center of the primary peak, support the morphology of hexagonally packed cylinders (HEX) with PS cylinders in PEB matrix for the SEBS sample (25 vol.% PS). After tethering the QA group to the PS block, the dry SEBS-$C_5$-TMA-0.8 sample showed broad scattering peaks at q/q* = 1 and √4, suggesting a morphological change from HEX to lamellar structures (LAM) (Figure 3a). This change in microstructure is likely caused by the volume fraction increase of the PS domain in the overall composition: from 30 wt.% (25 vol.%) PS in pristine SEBS to 55 wt.% (45 vol.%) PS in SEBS-$C_5$-TMA-0.8 (density: 0.86 g/cm$^3$ for PEB, 1.05 g/cm$^3$ for PS, and 1.30 g/cm$^3$ for QA-functionalized PS[44]). The increase in PS domain volume fraction after the QA functionalization induced development of 2D lamellar layers from 1D cylindrical domains,[45] where the diameter of the PS cylinders and the thickness of QA-tethered PS lamella are similar. Furthermore, the main q* peak became broader after QA-tethering onto the SEBS. This broadening is due to the *intermolecular linking* of the PEB chains during the Friedel-Crafts reaction, which caused an increase in $M_n$ and must have caused chain packing frustrations to hinder the formation of a well-defined LAM morphology. This *intermolecular linking* and possible kinetic trapping during solution casting may have caused the SEBS-$C_5$-TMA-0.8 sample to yield a less ordered microstructure in SAXS and TEM measurements (Figure 3b). The hydrated SEBS-$C_5$-TMA-0.8 sample showed peaks in the SAXS profile at 1, √3, and √4, suggesting formation of an inverted hexagonally packed cylindrical structure, where the hydrophobic PEB block formed cylindrical domains in the matrix of hydrated QA-tethered PS. We believe that hydration of the QA-tethered PS (*e.g.* WU of SEBS-$C_5$-TMA-0.8 is 150 wt.%) domain increased the overall volume fraction of hydrophilic domains, which caused formation of the inverted hexagonally packed cylindrical morphology. The microstructure of crosslinked SEBS AEMs was also investigated by SAXS. As the degree of crosslinking increased, the interdomain spacing of the AEMs decreased (Figure S15).

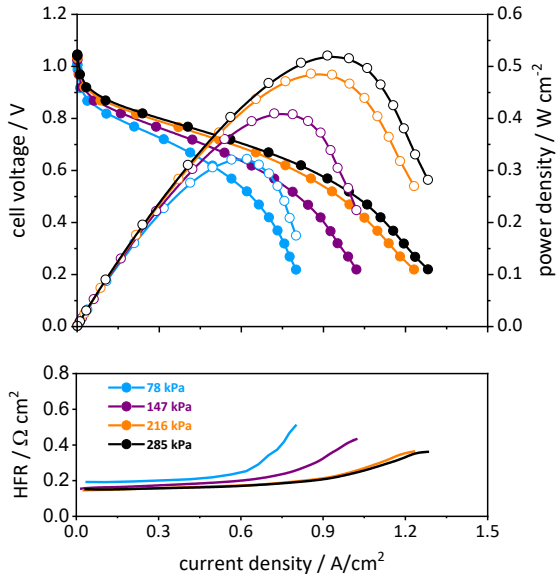


**Figure 4.** AEM fuel cell performance of an MEA employing the XL100-SEBS-$C_5$-TMA-0.8 membrane at 60 °C as a function of backpressure. (Anode: PtRu/C (0.5 mg$_{Pt}$/cm$^2$), Cathode: Pt/C (0.6 mg$_{Pt}$/cm$^2$), membrane thickness: 60 μm, under fully humidified $H_2/O_2$ gases).

**AEM Fuel Cell Performance.** The performance of a crosslinked SEBS AEM was evaluated in fuel cell testing. Figure 4 shows the polarization curves, power density and high-frequency resistance (HFR) of an MEA using the XL100-SEBS-C5-TMA-0.8 membrane at 60 °C as a function of backpressure. The performance of the cell improved as the backpressure of the reactant gases increased from 78 to 285 kPa, indicating that the SEBS-based MEA did not have electrode flooding issues. The HFR of the cell at low current density (*ca.* < 0.6 A cm$^{-2}$) was ~0.15 Ω cm$^2$, in good agreement with the value calculated from the hydroxide conductivity and thickness of the membrane (41 mS cm$^{-1}$, 60 μm). This result indicates that the interfacial resistance between the membrane and electrode was negligible due to the low water uptake of the crosslinked membrane.[46] At higher current densities, HFR tended to increase quickly likely due to the cathode dry-out from poor back-diffusion of water from the anode to the cathode. Although there are a few reports demonstrating peak power density of 1–2 W cm$^{-2}$ recently,[47-49] the peak power density of 520 mW cm$^{-2}$ for this SEBS-based MEA is the highest level among those of other reported SEBS-based MEAs.[30,31,43] Further improved performance is expected with more optimized membranes including thinner samples with higher water transport.

## CONCLUSIONS

A new synthetic method based on bromoalkylation was developed for the convenient preparation of alkyl-tethered QA aromatic polymer AEMs. This acid-catalyzed Friedel-Crafts reaction with a bromoalkylated *tertiary* alcohol effectively functionalized the PS block of SEBS (up to 95% DF) and enabled elastic AEMs with various tether lengths and IECs. Subsequent

amination/crosslinking generated SEBS AEMs with good elastic mechanical properties that are critical for practical use in AEM fuel cells. AEM structures with a long tethered cation head group and all-carbon backbone afforded good alkaline stability. The morphology measurements on these materials indicated that the increase in volume fraction of the PS domain upon functionalization affected the microstructure of SEBS, changing the material's morphology from a hexagonally packed cylindrical structure to a less ordered lamellar structure in agreement with coarse-grained simulations.[45] When AEM fuel cell performance was evaluated with a crosslinked SEBS AEM sample, a peak power density of 520 mW/cm$^2$ was achieved at 60 °C with $H_2/O_2$ reactant gases. This convenient polymer functionalization approach will serve as a versatile synthetic method to prepare stable aromatic AEMs with a wide range of chemical structures.

## EXPERIMENTAL SECTION

**Instrumentation.** $^1$H NMR spectra were obtained with a Varian Unity 500 MHz spectrometer, and chemical shifts were referenced to the residue solvent peaks; $CDCl_3$ (at 7.26 ppm). Number- and weight-average molecular weights of polymers were determined by a size exclusion chromatography (SEC) on a Viscotek T60A instrument with differential refractive index detector (Viscotek 302), using THF as eluent and polystyrene as standard. Small angle x-ray scattering (SAXS) experiments were conducted at 5-ID beamline at the Advanced Photon Source (Argonne National Laboratory, IL, USA). The typical operating conditions were set as follows: a wavelength of $\lambda$ = 0.7293 Å$^{-1}$, a beam size of 0.5 x 1 mm$^2$, a sample-to-detector distance of 8.503 m.[50] The SAXS profiles were recorded by a Rayonix CCD area detector with dimensions of 170 x 170 mm$^2$. For transmission electron microscopy (TEM) characterization, ultrathin (~60 nm) specimens of membrane were prepared at -50 °C using a CRX-PTXL cryo-ultramicrotome (RMC) with a diamond knife. The aromatic ring of styrene block in the membrane was selectively stained with $RuO_4$ at room temperature to enhance the electron density contrast. TEM was operated using JEM-2010 (JEOL) with an acceleration voltage of 200 kV to observe the morphology. Stress-strain behavior was measured by dynamic mechanical analyzer (TA Q800 DMA). The temperature and humidity were controlled in a humidity chamber (DMA-RH Accessory). The membrane sample (20 mm × 5 mm × 0.05 mm) was used in all tests.

**Materials.** Polystyrene-*b*-poly(ethylene-*co*-butylene)-*b*-polystyrene [SEBS; $M_w$ = 105 kg/mol, polydispersity index (PDI) = 1.04 measured from SEC using THF as eluent] was purchased from Sigma Aldrich. The SEBS contains 30 wt% (or 18 mol%) styrene units, and its composition was confirmed by NMR spectroscopy. All reagents and solvents were purchased from Sigma-Aldrich, Alfa Aesar and Acros Organics, and were used without further purification.

**7-Bromo-2-methylheptan-2-ol.** This procedure is based on a modified literature report.[51] Ethyl 6-bromohexanoate (25.0 g, 112 mmol) and anhydrous diethyl ether (90 mL) were added to a 500 mL round bottom flask in inert condition. After cooling in an ice bath, $CH_3MgBr$ solution (3 M in ether, 75 mL, 224 mmol) was added to the round bottom flask dropwise by a dropping funnel. The ice bath was then removed and the reaction mixture was stirred at room temperature for 4 h. The reaction was slowly quenched with saturated $NH_4Cl$ aq. (60 mL) and water (50 mL). The product was extracted with diethyl ether (2 x 50 mL), dried over $MgSO_4$, and concentrated on a rotary evaporator. The pure product was isolated as a colorless liquid (23.0 g, 98% yield).

**6-Bromo-2-methylhexan-2-ol** was synthesized using the same procedure for 7-bromo-2-methylheptan-2-ol with methyl 5-bromovalerate (12 g, 61.5 mmol). The product was isolated as a colorless liquid (11.5 g, 96% yield).

**5-Bromo-2-methylpentan-2-ol** was synthesized using the same procedure for 7-bromo-2-methylheptan-2-ol with methyl 4-bromobutyrate (10 g, 51.3 mmol). The product was isolated as a colorless liquid (7.59 g, 82% yield).

**Preparation of SEBS-C$_n$-Br-0.8.** The following is a representative procedure for acid catalyzed Friedel-Crafts bromoalkylation. To a 50 mL Schlenk flask was added SEBS (1.0 g, 2.79 mmol styrene units) and 7-bromo-2-methylheptan-2-ol (0.58 g, 2.79 mmol, 1.0 eq. per styrene unit). The flask was evacuated and purged with nitrogen. Anhydrous dichloromethane (20 mL) was added using a syringe and the solution was stirred until SEBS is dissolved. After cooling the flask in an ice bath, triflic acid (0.27 mL, 3.07 mmol, 1.1 eq.) was added using a syringe. The reaction mixture was stirred at 0 °C for 1 h, after which the reaction was poured into methanol to precipitate the polymer. The white polymer was filtered, redissolved in tetrahydrofuran, and precipitated in methanol. The polymer product was isolated after vacuum drying at room temperature (1.4 g, 98% yield). Based on $^1$H NMR analysis, 80% of styrene units were functionalized.

**Preparation of SEBS-C$_n$-TMA-0.8 membrane.** The following is a representative procedure for amination. SEBS-C$_5$-Br-0.8 (0.18 g) was dissolved in toluene (4 mL), filtered, and cast onto a glass plate. The dry SEBS-C$_5$-Br-0.8 film (approximately 40 μm thick) was immersed in aqueous trimethylamine (45 wt% in water) at 45 °C for 48 h. The film was rinsed with water and ion exchanged to hydroxide form by immersing in 1M NaOH at room temperature for 48 h in an argon-filled glovebox.

**Preparation of XL20-SEBS-C$_n$-TMA-0.8 membrane.** The following is a representative procedure for XLy-SEBS-C$_n$-TMA-0.8. SEBS-C$_5$-Br-0.8 (0.30 g, 0.462 mmol of Br) and *N*,*N*,*N*',*N*'-tetramethyl-1,6-hexanediamine (8.0 mg, 0.0462 mmol) were dissolved in THF (6 mL) and stirred at room temperature for 2 h. The mixture was filtered and cast onto a glass plate. Once it is dried, the crosslinked membrane was immersed in aqueous trimethylamine (45 wt% in water) at 45°C for 48 h. The film was rinsed with water and ion exchanged to hydroxide form by immersing in 1M NaOH at room temperature for 48 h in an argon-filled glovebox.

**Ion Exchange Capacity (IEC).** IECs of membranes in bromide anion form were determined by Mohr titration. About 0.15 g of membrane was dried at 50 °C in vacuum for 24 h and weighed. The membrane in bromide form was immersed in 20 mL of a 0.5 M $NaNO_3$ solution for 48 h. The $NaNO_3$ solution was titrated with a 0.1 M $AgNO_3$ using $K_2CrO_4$ as a colorimetric indicator. IEC was calculated from dry mass of the membrane and the amount $AgNO_3$ consumed in titration.

**Water Uptake, Hydration Number, and Swelling Degree.** In an argon-filled glovebox, fully hydrated AEMs (in hydroxide form) were taken out of water, blotted quickly with a KimWipe to remove surface liquid, and weighed immediately. The membranes were then dried at 50 °C under vacuum for 24 h and weighed again. Water uptake (%) was calculated from:

$$\text{Water uptake (\%)} = [(W_{wet} - W_{dry}) \times 100] / W_{dry}$$

where $W_{wet}$ and $W_{dry}$ are the weight of the water-swollen and the corresponding dry membranes, respectively. The hydration

number (λ), which represents the average number of water molecules per quaternary ammonium group, was calculated as:

$$\lambda = [(W_{wet} - W_{dry}) / W_{dry}] \times [1000 / M_{H2O}IEC]$$

where $M_{H2O}$ is the molecular mass of water (18 g/mol).

The in-plane swelling was characterized by the linear expansion ratio, which was calculated by the ratio of difference between the wet and dry dimensions to the dry dimensions:

$$\text{Swelling degree (\%)} = [(X_{wet} - X_{dry}) \times 100] / X_{dry}$$

**Ion Conductivity Measurement.** Ion conductivities (σ in mS/cm) of each membrane (approximate size: 3 cm × 0.5 cm) were measured using a four-point probe method with BT-512 membrane conductivity test system (BekkTech LLC). Measurements were carried out under fully hydrated conditions at 30, 60, and 80 °C while the cell was fully immersed in deionized water. The cell was degassed first and blanketed with a flow of argon gas during entire measurement. At a given temperature, each membrane sample was equilibrated at least 90 min before recording measurements. Ionic conductivity was calculated according to:

$$\sigma\ (\text{mS/cm}) = \frac{L}{R \times W \times T}$$

where L is the distance between the two inner platinum wires (0.425 cm), R is the resistance of the membrane in Ω, and W and T are the width and thickness of the membrane in centimeters, respectively.

**Alkaline Stability Test.** The alkaline stability of the SEBS AEMs were measured by immersing the membranes (5 cm x 2.5 cm) in 1M NaOH aq. solution at 80°C for 500 h. After 500 h, membranes were washed by immersion in distilled water 3 times for 2 days, and the counter anion was exchanged to $Cl^-$ to measure the IEC by Mohr titration. Alkaline stability was confirmed by comparing hydroxide ion conductivity and titrated IECs (Table 2), FT-IR (Figures S3–S5), elemental analysis (Table S3), and mechanical properties (Figures S9–S13) of aged and unaged samples.

**AEM Fuel Cell Performance.** The anode and cathode of the MEA were fabricated from PtRu/C (1:1 Pt:Ru, 75% metal on high surface area carbon, HISPEC 12100 catalyst, Johnson Matthey) and Pt/C (60% Pt on high surface area carbon, HISPEC 9100 catalyst, Johnson Matthey), respectively. The catalyst ink was formulated from catalyst powder, poly(fluorene) ionomer (FLN) and 80:20 isopropanol/water solution. The detailed synthesis of the FLN ionomer is reported elsewhere.[49] The catalyst inks were then brush painted on the gas diffusion layer (GDL, BC-29, SGL Carbon) at 60 °C under constant vacuum to form electrodes. The Pt loading and ionomer to catalyst ratio were 0.5 mg/cm$^2$, 52% and 0.6 mg/cm$^2$, 40% for anode and cathode, respectively. The MEA was fabricated by sandwiching the membrane between the anode and cathode gas diffusion layers. The MEA was placed into fuel cell hardware (5 cm$^2$ active area) and 40 psi of torque was applied to compress the MEA. The polarization curves were obtained after a break-in at 60 °C overnight with flow rates for $H_2$ and $O_2$ of 2000 and 1000 sccm, respectively.

## ASSOCIATED CONTENT

### Supporting Information

The Supporting Information is available free of charge on the ACS Publications website at http://pubs.acs.org.

## AUTHOR INFORMATION


### Corresponding Author

* E-mail: baec@rpi.edu.

### ORCID

Chulsung Bae: 0000-0002-9026-3319


### Notes

The authors declare no competing financial interest.

## ACKNOWLEDGMENT


This work was supported by the National Science Foundation (CHE 1534289) and U.S. Department of Energy (ARPA-E, IONICS DE-AR0000769). The authors gratefully acknowledge research support from the HydroGEN Advanced Water Splitting Materials Consortium, established as part of the Energy Materials Network under the U.S. Department of Energy, Office of Energy Efficiency and Renewable Energy, Fuel Cell Technologies Office, under Contract Number DE-AC52-06NA25396 (Los Alamos National Laboratory). Portions of this work were performed at the DuPont–Northwestern–Dow Collaborative Access Team (DND-CAT) located at Sector 5 of the Advanced Photon Source (APS). Use of the APS, an Office of Science User Facility of US Department of Energy operated by Argonne National Laboratory, was supported by the US DOE under Contract DE-AC02-06CH11357.


## REFERENCES


(1) Hickner, M. A.; Herring, A. M.; Coughlin, E. B. Anion exchange membranes: Current status and moving forward. *J. Polym. Sci., Part B: Polym. Phys.* **2013,** *51*, 1727-1735.

(2) Varcoe, J. R.; Atanassov, P.; Dekel, D. R.; Herring, A. M.; Hickner, M. A.; Kohl, P. A.; Kucernak, A. R.; Mustain, W. E.; Nijmeijer, K.; Scott, K.; Xu, T.; Zhuang, L. Anion-exchange membranes in electrochemical energy systems. *Energy Environ. Sci.* **2014,** *7*, 3135-3191.

(3) Maurya, S.; Shin, S.-H.; Kim, Y.; Moon, S.-H. A review on recent developments of anion exchange membranes for fuel cells and redox flow batteries. *RSC Adv.* **2015,** *5*, 37206-37230.

(4) Li, N.; Guiver, M. D. Ion Transport by Nanochannels in Ion-Containing Aromatic Copolymers. *Macromolecules* **2014,** *47*, 2175-2198.

(5) Dekel, D. R. Review of cell performance in anion exchange membrane fuel cells. *J. Power Sources* **2018**, 375, 158-169.

(6) Gottesfeld, S.; Dekel, D. R.; Page, M.; Bae, C.; Yan, Y.; Zelenay, P.; Kim, Y. S. Anion exchange membrane fuel cells: Current status and remaining challenges. *J. Power Sources* **2018,** *375*, 170-184.

(7) Pan, J.; Lu, S.; Li, Y.; Huang, A.; Zhuang, L.; Lu, J. High-Performance Alkaline Polymer Electrolyte for Fuel Cell Applications. *Adv. Funct. Mater.* **2010,** *20*, 312-319.

(8) Tanaka, M.; Fukasawa, K.; Nishino, E.; Yamaguchi, S.; Yamada, K.; Tanaka, H.; Bae, B.; Miyatake, K.; Watanabe, M. Anion Conductive Block Poly(arylene ether)s: Synthesis, Properties, and Application in Alkaline Fuel Cells. *J. Am. Chem. Soc.* **2011,** *133*, 10646-10654.

(9) Mohanty, A. D.; Lee, Y.-B.; Zhu, L.; Hickner, M. A.; Bae, C. Anion Exchange Fuel Cell Membranes Prepared from C–H Borylation and Suzuki Coupling Reactions. *Macromolecules* **2014,** *47*, 1973-1980.

(10) Wang, J.; Wang, J.; Zhang, S. Synthesis and characterization of cross-linked poly(arylene ether ketone) containing pendant quaternary ammonium groups for anion-exchange membranes. *J. Membr. Sci.* **2012,** *415–416*, 205-212.

(11) Zhu, L.; Zimudzi, T. J.; Wang, Y.; Yu, X.; Pan, J.; Han, J.; Kushner, D. I.; Zhuang, L.; Hickner, M. A. Mechanically Robust Anion Exchange Membranes *via* Long Hydrophilic Cross-Linkers. *Macromolecules* **2017,** *50*, 2329-2337.

(12) Dang, H.; Jannasch, P. A comparative study of anion-exchange membranes tethered with different hetero-cycloaliphatic quaternary ammonium hydroxides. *J. Mater. Chem. A* **2017,** *5,* 21965-21978.

(13) Fujimoto, C.; Kim, D.-S.; Hibbs, M.; Wrobleski, D.; Kim, Y. S. Backbone stability of quaternized polyaromatics for alkaline membrane fuel cells. *J. Membr. Sci.* **2012,** *423–424*, 438-449.

(14) Mohanty, A. D.; Tignor, S. E.; Krause, J. A.; Choe, Y.-K.; Bae, C. Systematic Alkaline Stability Study of Polymer Backbones for Anion Exchange Membrane Applications. *Macromolecules* **2016,** *49*, 3361-3372.

(15) Hibbs, M. R.; Fujimoto, C. H.; Cornelius, C. J. Synthesis and Characterization of Poly(phenylene)-Based Anion Exchange Membranes for Alkaline Fuel Cells. *Macromolecules* **2009,** *42*, 8316-8321.

(16) Lee, W.-H.; Kim, Y. S.; Bae, C. Robust Hydroxide Ion Conducting Poly(biphenyl alkylene)s for Alkaline Fuel Cell Membranes. *ACS Macro Lett.* **2015,** *4*, 814-818.

(17) Lee, W.-H.; Park, E. J.; Han, J.; Shin, D. W.; Kim, Y. S.; Bae, C. Poly(terphenylene) Anion Exchange Membranes: The Effect of Backbone Structure on Morphology and Membrane Property. *ACS Macro Lett.* **2017,** *6*, 566-570.

(18) Olsson, J. S.; Pham, T. H.; Jannasch, P. Poly(arylene piperidinium) Hydroxide Ion Exchange Membranes: Synthesis, Alkaline Stability, and Conductivity. *Adv. Funct. Mater.* **2018,** *28*, 1702758.

(19) Park, E. J.; Kim, Y. S., Quaternized aryl ether-free polyaromatics for alkaline membrane fuel cells: synthesis, properties, and performance – a topical review. *J. Mater. Chem. A* **2018,** *6*, 15456-15477.

(20) Pan, J.; Chen, C.; Li, Y.; Wang, L.; Tan, L.; Li, G.; Tang, X.; Xiao, L.; Lu, J.; Zhuang, L. Constructing ionic highway in alkaline polymer electrolytes. *Energy Environ. Sci.* **2014,** *7*, 354-360.

(21) Li, N.; Yan, T.; Li, Z.; Thurn-Albrecht, T.; Binder, W. H. Comb-shaped polymers to enhance hydroxide transport in anion exchange membranes. *Energy Environ. Sci.* **2012,** *5*, 7888-7892.

(22) Wang, C.; Li, N.; Shin, D. W.; Lee, S. Y.; Kang, N. R.; Lee, Y. M.; Guiver, M. D. Fluorene-Based Poly(arylene ether sulfone)s Containing Clustered Flexible Pendant Sulfonic Acids as Proton Exchange Membranes. *Macromolecules* **2011,** *44*, 7296-7306.

(23) Wang, C.; Young Lee, S.; Won Shin, D.; Rae Kang, N.; Lee, Y. M.; Guiver, M. D. Proton-conducting membranes from poly(ether sulfone)s grafted with sulfoalkylamine. *J. Membr. Sci.* **2013,** *427*, 443-450.

(24) Ran, J.; Wu, L.; Xu, T. Enhancement of hydroxide conduction by self-assembly in anion conductive comb-shaped copolymers. *Polym. Chem.* **2013,** *4*, 4612-4620.

(25) Dang, H.-S.; Jannasch, P. Exploring Different Cationic Alkyl Side Chain Designs for Enhanced Alkaline Stability and Hydroxide Ion Conductivity of Anion-Exchange Membranes. *Macromolecules* **2015,** *48*, 5742-5751.

(26) Lin, C. X.; Huang, X. L.; Guo, D.; Zhang, Q. G.; Zhu, A. M.; Ye, M. L.; Liu, Q. L. Side-chain-type anion exchange membranes bearing pendant quaternary ammonium groups *via* flexible spacers for fuel cells. *J. Mater. Chem. A* **2016,** *4*, 13938-13948.

(27) Vinodh, R.; Ilakkiya, A.; Elamathi, S.; Sangeetha, D. A novel anion exchange membrane from polystyrene (ethylene butylene) polystyrene: Synthesis and characterization. *Mater. Sci. Eng., B* **2010,** *167*, 43-50.

(28) Zeng, Q. H.; Liu, Q. L.; Broadwell, I.; Zhu, A. M.; Xiong, Y.; Tu, X. P. Anion exchange membranes based on quaternized polystyrene-*block*-poly(ethylene-*ran*-butylene)-*block*-polystyrene for direct methanol alkaline fuel cells. *J. Membr. Sci.* **2010,** *349*, 237-243.

(29) Sun, L.; Guo, J.; Zhou, J.; Xu, Q.; Chu, D.; Chen, R. Novel nanostructured high-performance anion exchange ionomers for anion exchange membrane fuel cells. *J. Power Sources* **2012,** *202*, 70-77.

(30) Mohanty, A. D.; Ryu, C. Y.; Kim, Y. S.; Bae, C. Stable Elastomeric Anion Exchange Membranes Based on Quaternary Ammonium-Tethered Polystyrene-*b*-poly(ethylene-*co*-butylene)-*b*-polystyrene Triblock Copolymers. *Macromolecules* **2015,** *48*, 7085-7095.

(31) Lin, C. X.; Wang, X. Q.; Hu, E. N.; Yang, Q.; Zhang, Q. G.; Zhu, A. M.; Liu, Q. L. Quaternized triblock polymer anion exchange membranes with enhanced alkaline stability. *J. Membr. Sci.* **2017,** *541*, 358-366.

(32) Hibbs, M. R. Alkaline stability of poly(phenylene)-based anion exchange membranes with various cations. *J. Polym. Sci., Part B: Polym. Phys.* **2013,** *51*, 1736-1742.

(33) Nakahara, A.; Satoh, K.; Kamigaito, M. Cycloolefin Copolymer Analogues from Styrene and Isoprene: Cationic Cyclization of the Random Copolymers Prepared by Living Anionic Polymerization. *Macromolecules* **2009,** *42*, 620-625.

(34) Dynamic mechanical analyzer with humidity chamber has 350-400% of the maximum elongation range (TA Q800-RH).

(35) Tsai, T. H.; Ertem, S. P.; Maes, A. M.; Seifert, S.; Herring, A. M.; Coughlin, E. B. Thermally Cross-Linked Anion Exchange Membranes from Solvent Processable Isoprene Containing Ionomers. *Macromolecules* **2015,** *48*, 655-662.

(36) Varcoe, J. R.; Slade, R. C. T.; Lam How Yee, E. An alkaline polymer electrochemical interface: a breakthrough in application of alkaline anion-exchange membranes in fuel cells. *Chem. Comm.* **2006,** 1428-1429.

(37) Park, J. S.; Park, S. H.; Yim, S. D.; Yoon, Y. G.; Lee, W. Y.; Kim, C. S. Performance of solid alkaline fuel cells employing anion-exchange membranes. *J. Power Sources* **2008,** *178*, 620-626.

(38) Park, A. M.; Wycisk, R. J.; Ren, X.; Turley, F. E.; Pintauro, P. N. Crosslinked poly(phenylene oxide)-based nanofiber composite membranes for alkaline fuel cells. *J. Mater. Chem. A* **2016,** *4*, 132-141.

(39) Zhu, L.; Zimudzi, T. J.; Li, N.; Pan, J.; Lin, B.; Hickner, M. A. Crosslinking of comb-shaped polymer anion exchange membranes via thiol–ene click chemistry. *Polym. Chem.* **2016,** *7*, 2464-2475.

(40) Ertem, S. P.; Tsai, T. H.; Donahue, M. M.; Zhang, W.; Sarode, H.; Liu, Y.; Seifert, S.; Herring, A. M.; Coughlin, E. B. Photo-Cross-Linked Anion Exchange Membranes with Improved Water Management and Conductivity. *Macromolecules* **2016,** *49*, 153-161.

(41) Wang, L.; Hickner, M. A. Low-temperature crosslinking of anion exchange membranes. *Polym. Chem.* **2014,** *5*, 2928-2935.

(42) Dai, P.; Mo, Z.-H.; Xu, R.-W.; Zhang, S.; Wu, Y.-X., Cross-Linked Quaternized Poly(styrene-b-(ethylene-co-butylene)-b-styrene) for Anion Exchange Membrane: Synthesis, Characterization and Properties. *ACS Appl. Mater. Interfaces* **2016,** *8*, 20329-20341.

(43) Hao, J.; Gao, X.; Jiang, Y.; Zhang, H.; Luo, J.; Shao, Z.; Yi, B. Crosslinked high-performance anion exchange membranes based on poly(styrene-b-(ethylene-co-butylene)-b-styrene). *J. Membr. Sci.* **2018,** *551*, 66-75.

(44) The density of QA functionalizaed PS was measured by pycnometer.

(45) Sepehr, F.; Liu, H.; Luo, X.; Bae, C.; Tuckerman, M. E.; Hickner, M. A.; Paddison, S. J. Mesoscale Simulations of Anion Exchange Membranes Based on Quaternary Ammonium Tethered Triblock Copolymers. *Macromolecules* **2017,** *50*, 4397-4405.

(46) Kim, Y. S.; Pivovar, B. S. The Membrane–Electrode Interface in PEFCs IV. The origin and implications of interfacial resistance. *J. Electrochem. Soc.* **2010**, 157, B1616-B1623.

(47) Wang, L.; Bellini, M; Miller, H. A.; Varcoe, J. R. A high conductivity ultrathin anion-exchange membrane with 500+ h alkali stability for use in alkaline membrane fuel cells that can achieve 2 W $cm^{-2}$ at 80 °C. *J. Mater. Chem. A* **2018,** *6*, 15404-15412.

(48) Wang, Y.; Wang, G.; Li, G.; Huang, B.; Pan, J.; Liu, Q.; Han, J.; Xiao, L.; Lua, J.; Zhuang, L. Pt–Ru catalyzed hydrogen oxidation in alkaline media: oxophilic effect or electronic effect? *Energy Environ. Sci.* **2015,** *8*, 177-181.

(49) Maurya, S.; Noh, S.; Matanovic, I.; Park, E. J.; Narvaez Villarrubia, C.; Han, J.; Bae, C.; Kim, Y. S. Rational design of polyaromatic ionomers for alkaline membrane fuel cells with >1 W $cm^{-2}$ power density. *Energy Environ. Sci.* **2018**, in press (DOI: 10.1039/C8EE02192A).

(50) Weigand, S. J.; Keane, D. T. DND-CAT's new triple area detector system for simultaneous data collection at multiple length scales. *Nucl. Instr. Meth. Phys. Res. A.* **2011,** *649*, 61-63.

(51) Fauq, A. H.; Kache, R.; Khan, M. A.; Vega, I. E. Synthesis of Acid-Cleavable Light Isotope-Coded Affinity Tags (ICAT-*L*) for Potential Use in Proteomic Expression Profiling Analysis. *Bioconjug. Chem.* **2006,** *17*, 248-254.

Table of Contents artwork